International Journal of Communication Networks and Information Security
ISSN: 2073-607X, 2076-0930
Volume 14 Issue 02 Year 2022 Page 261:272

Climate Change Analysis Based on Satellite Multispectral Image Processing in Feature Selection Using Reinforcement Learning

Muhammad Yus Firdaus[1*], Mustofa Kamil[2]
[1]*Universitas Islam Syeikh Yusuf, Tangerang, Banten, Indonesia*
[2]*Universitas Pendidikan Indonesia, Bandung, West Java, Indonesia*
[1]*muhammadyusfir@outlook.com*, [2]*muskamil14@gmail.com*
https://orcid.org/0000-0002-2424-1410, https://orcid.org/0000-0002-9692-8238
[*]*Corresponding Author: Muhammad Yus Firdaus*

Article History

Received: 24 March 2022
Revised: 28 July 2022
Accepted: 29 August 2022

Abstract

Currently private and government agencies use remote sensing images (RSI) for various applications from military applications to agriculture growth. The images can be multispectral, panchromatic, ultra-spectral, or hyperspectral of terra bytes. RSI classification is considered one important application for remote sensing. Climate change detection especially affects numerous aspects of day-to-day lives, for instance, forestry management, weather forecasting, transportation, agriculture, road condition monitoring, and the detection of the natural atmosphere. Conversely, certain research works had a focus on classification of actual weather phenomenon images, generally depending on visual observations from humans. The conventional artificial visual difference between weather phenomena will take more time and error-prone. This paper develops a new reinforcement learning based climate change analysis on satellite multispectral image processing (RLCCA-SMSIP) technique. In order to properly determine climate change, the RLCCA-SMSIP technique employs residual network (ResNet-101) model for feature extraction. Next, deep reinforcement learning (DRL) approach is utilized for climate classification. Finally, parameter selection of the RLCCA-SMSIP technique involves sine cosine algorithm (SCA) for DRL model. For assuring the enhanced outcomes of the presented RLCCA-SMSIP model, comprehensive comparison results are assessed. The obtained values denote the supremacy of the RLCCA-SMSIP model on climate classification.

Keywords: Reinforcement learning; Satellite images; Climate change; Deep learning, Parameter selection

1.Introduction

The examination of climate phenomena assumes a pivotal part in different applications, for instance, nature observing, climate gauging, and the evaluation of ecological quality. Furthermore, unique climate peculiarities differently affect farming [1]. Consequently, precisely recognizing climate peculiarities can work on farming preparation. Besides, climate peculiarities not just emphatically impact vehicle partner driving frameworks (by snow, dust storm, dimness, and so on) yet additionally influences us in our day-to-day routines, like the wearing, voyaging, and sun oriented advancements.

In the interim, the usefulness of numerous visual frameworks like open air video reconnaissance is additionally impacted by climate peculiarities. Furthermore, the climate peculiarities (cloudiness, snow, dust storm, etc) that happened the day preceding will likewise influence climate conditions for the following couple of days. Neighbourhood or provincial climate conditions like dust storms, weighty downpour, rime, snow, murkiness, and agglomerate haze are perilous climate conditions that could be part of the way liable for an enormous number of car crashes on interstates [2]. In this way, we can arrive at the basic resolution that the arrangement of climate peculiarities is fundamental and can assist meteorologists with understanding climatic circumstances, as well as further, develop climate determining.

As of late, there has been an expansion in interest in the general population for the biological system encompassing people. Frequently, it is accepted that a more profound comprehension of the natural setting one lives in makes them bound to advocate for ecological activism, and along these lines, developing this expanded interest is significant [3]. Disregarding this, it is once in a while hard to more deeply study the environment around an area without master help, particularly when one doesn't have the particular jargon to depict the biological system. One method for improving this is by giving the climate grouping to a particular picture. In spite of the fact that climate isn't the main variable that describes an environment, a straightforward snippet of data gives a leaping off highlight get familiar with the regular world overall [4]. Moreover, with the ascent of a worldwide temperature alteration, climate is a significant part of the framework, as various climates might change definitely from now on. At last, climate is a down to earth decision for state funded schooling, as framework, for example, the Köppen-Geiger climate orders are very much organized and characterized.

Remote Sensing (RS) pictures contain enormous measure of data and in the event that the picture quality isn't great or on the other hand in the event that the picture examination doesn't utilize ideal list of capabilities, then, at that point, the effect of RS application for which the strategy is utilized may not be completely used [5]. The visual translation of RS pictures uses various components of understanding like shape, shade, tone, surface, etc. Physically understanding is restricted to examining just single picture at a time due to the trouble in numerous picture translations. Manual translation is emotional and time for visual arrangement relies fundamentally upon the picture quality. This has cleared way for programmed handling over visual examination and is helpful for concurrent investigation of numerous unearthly groups and can deal with huge informational indexes a lot quicker than people. So picture handling devices play a significant in applications relating to RS [6]. RS techniques are considered a reciprocal device in different applications because of the extensive variety of regions the pictures can cover. The handiness of satellite pictures to RS applications relies upon the precision of the methods. A decent comprehension of how well the picture handling strategies perform will help in choosing the most ideal selection of techniques for different applications. With the upgrade of innovation, interest for close ongoing checking and visual pictures for use in crisis administrations and the general population on account of a catastrophic event is expanding. Late headways in earth checking satellites are clearing a path towards use in such applications [7]. Techniques are subsequently being created to use the accessible information successfully to ensure that the most ideal knowledge is accessible to crisis administrations and leaders on time. While a tremendous measure of computerized satellite and ethereal symbolism is accessible, the genuine test is in the examination of crude pictures, extraction of valuable data with high precision, and applying it to certifiable directions and applications. Despite the fact that there are different picture handling strategies accessible, traditional techniques should be basically looked into and picture understanding concerning elements of interest is significant [8]. With the advances in man-made brainpower and machine learning, there is an improvement in extraction of itemized highlights from high goal elevated symbolism. The blade's various layers are used for creating different picture handling procedures.

By and large, conventional order techniques for climate peculiarities depend on human perception. Notwithstanding, the conventional fake visual differentiation between climate peculiarities takes a great deal of time and is inclined to blunders. Consequently, there is a pressing need to foster high-accuracy, productive, and computerized advancements for climate peculiarities arrangement [9]. The term machine learning (ML) was authored in 1959 and characterized as "the field of study that gives PCs the capacity to learn without being expressly modified for that". Thus, ML has zeroed in on the

improvement of calculations that permit scientists to streamline an exhibition measure utilizing verifiable information and experience. Throughout the long term, the ML field has been developing, principally because of its capacity to deal with gigantic measures of information and concentrate pertinent data from it, its special qualities relating to order and anticipating, and the development of computational power [10]. In this manner, it has been setting out new open doors for a few fields and applications (e.g., climate change, biodiversity crumbling, land-use change (e.g., deforestation), catastrophic events, arising sicknesses and other wellbeing gambles and the executives of normal assets), including regions that utilization EO information.

This paper develops a new reinforcement learning based climate change analysis on satellite multispectral image processing (RLCCA-SMSIP) technique. In order to properly determine climate change, the RLCCA-SMSIP technique employs residual network (ResNet-101) model for feature extraction. Next, deep reinforcement learning (DRL) approach is utilized for climate classification. Finally, parameter selection of the RLCCA-SMSIP technique involves sine cosine algorithm (SCA) for DRL model. For assuring the enhanced outcomes of the presented RLCCA-SMSIP model, comprehensive comparison results are assessed.

2. Literature Review

In [11], ML related technique to estimate solar radiation on earth external was offered. Toward strategy, the ML technique, multispectral (infrared and visible) satellite imageries of actual high-resolution after manifold positions stay as main data. The broadside particulars the complete process, counting feature selection, data collection, and pre-processing, along with the assortment of finest ML approaches, validation, and measurements. The effect of every input feature in approximating solar radiation was similarly scrutinized by means of connection techniques. Wang et al. [12] study snow coverage maps through learning from Sentinel-2 satellite multispectral images through ML approaches. The main dataset for snow attention mapping with 3 representative courses (background, snow, and cloud) was original labelled and composed through the semi-automatic classifier plugin in QGIS. Formerly, RF-related traditional ML and U-Net-related DL were every day to the semantic segmenting task in this labour.

Fu et al. [13] efforts to ferocity UAV imageries with spaceborne Jilin-1 (JL101K) multispectral imageries to classify vegetation societies of karst wetland by means of the optimized Light Gradient Boosting (LightGBM), RF, and XGBoost procedures. This training likewise quantitatively assesses image fusion quality after spectral fidelity, three-dimensional and detail travels the properties of dissimilar image feature groupings and techniques on mapping vegetation societies by dimensionality reduction and flexible selection. Oliveira et al. [14] devise to forecast sugarcane biometric variables through ML processes and multi-temporal information over the examination of multi-spectral images after drone onboard devices. The study has shown 5 diversities of sugar cane, since way to brand a healthy method. Multispectral images can be composed every fourteen days and the assessed biometric variables are the number of stalk diameter (SD), tillers (NT), and plant height (PH). Two ML techniques can be utilized they are random forest (RF) and multiple linear regression (MLR).

In [15], GaoFen-2 (GF-2) and Sentinel-2 images can be combined, and feature variable quantity and data states can be derivative by a projected adaptive feature variable combination optimization (AFCO) package to estimate the GSV of cone-bearing estates. The AFCO procedure has been associated with 4 old-style feature variable assortment approaches fast reiterative feature selection method for KNN (KNN-FIFS), RF, stepwise RF (SRF), and the feature variable showing and grouping optimized process related to the distance correlation coefficient and k-NN (DC-FSCK). Pontoglio et al. [16] purpose to validate how ML approaches are employed for automated feature extraction and detection in fluvial surroundings. The usage of photogrammetry and ML techniques has enhanced the sympathetic of both ecological and anthropical problems. The advanced method has been practiced as gaining multiple photogrammetric imageries cheers to UAV resounding multispectral cameras.

3. The Proposed Model

In this paper, a new RLCCA-SMSIP technique is developed for climate classification. In order to properly determine climate change, the RLCCA-SMSIP technique employs ResNet-101 model for feature extraction. Next, the DRL approach is utilized for climate classification. Finally, parameter selection of the RLCCA-SMSIP technique involves SCA for DRL model. Fig. 1 demonstrates the block diagram of RLCCA-SMSIP approach.

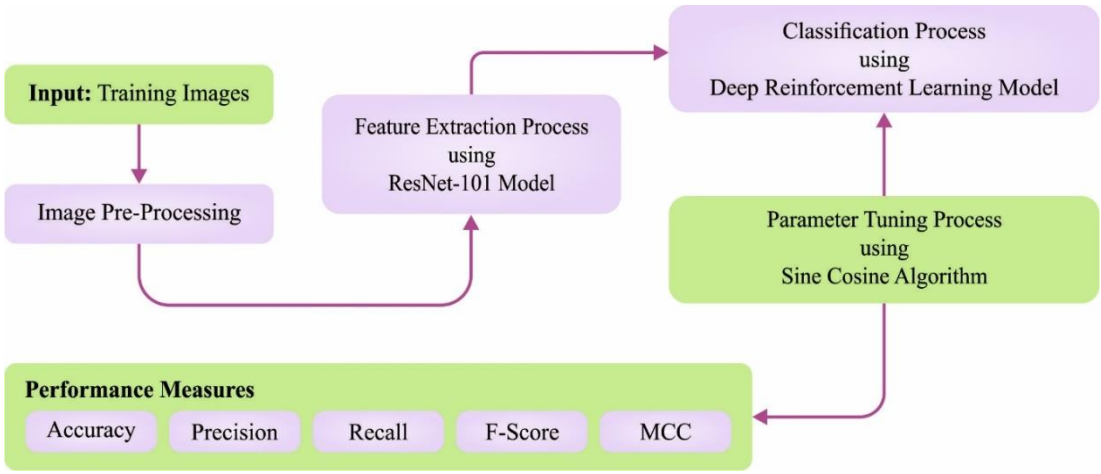

Figure 1. Block diagram of RLCCA-SMSIP approach

3.1. Feature Extraction

In order to properly determine climate change, the RLCCA-SMSIP technique employs ResNet-101 model for feature extraction. Data reliance is a crucial problem in DL. Compared with ML technique, an enormous quantity of information is required for training deep models. The major reason for these large number of training datasets is that it is essential to learn hidden patterns. But an enormous quantity of information is not frequently nearby for training a DL algorithm in some research fields, especially in medical imaging. The objective of TL model is to train a model using lesser information. There is no need for training the target models from scratch in TL.

Recently, DNN has made substantial development in the fields of image classification. In general, a deep model is an integration of lower, middle, and higher-level features, and a classifier. In this study, ResNet101 is used for extracting deep features. The VGG19 pre-trained network that is DCNN [17]. As previously stated, CNN model is composed of multiple layers that are interconnected with one another. Such layers are utilized for different tasks, namely medical image classification and natural language processing. The convolution filter size in ResNet101 is 33, and the stride value is 2. Down-sampling can be implemented in the convolution layer according to the stride value. These networks have 379 connections and 347 layers. The network input has dimension of 224 × 224 × 3. In the initial convolutional layer, the number of filters is 64, the filter size is [7, 7], and the number of channels is 3. The filter size in the max pooling layers is 3 × 3, and the stride value is 2. In the next convolution layer, the number of filters and channels is 64. In the last convolutional layer, the number of filters is 2048, with 512 channels. Later, obtain an output vector of dimension $N \times 2048$, whereas N represents the number of features, via extracting features from pool5 layer.

3.2. Climate Classification

Here, the DRL approach is utilized for climate classification. Deep learning empowers RL to scale to dynamic issues that were beforehand obstinate, i.e., settings with high-layered state and activity spaces. Among late work in the field of DRL, there have been two extraordinary examples of overcoming adversity [18]. The first, launching the transformation in DRL, was the improvement of a calculation that could figure out how to play a scope of Atari 2600 computer games at a godlike level, straightforwardly from picture pixels. Giving answers for the precariousness of capability estimate strategies in RL, this work was quick to convincingly show the way that RL specialists could be prepared on crude, high-layered perceptions, exclusively founded on a prize sign. The second champion

achievement was the improvement of a half breed DRL framework, AlphaGo, that crushed a human title holder in Go, resembling the memorable accomplishment of IBM's Deep Blue in chess twenty years sooner and IBM's Watson DeepQA framework that beat the best human Jeopardy! players. Dissimilar to the handmade standards that have ruled chess-playing frameworks, AlphaGo was made out of brain networks that were prepared utilizing directed and reinforcement learning, in blend with a customary heuristic pursuit calculation. Fig. 2 demonstrates the framework of DRL technique.

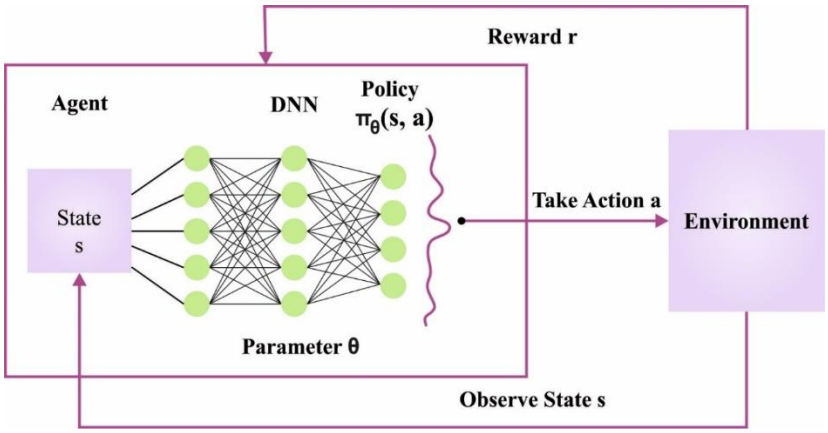

Figure 2. Architecture of DRL

DRL calculations have proactively been applied to many issues, like mechanical technology, where control approaches for robots can now be advanced straightforwardly from camera inputs, in reality, succeeding regulators that used to be hand engineered or gained from low-layered elements of the robot's state. In a stage towards considerably more fit specialists, DRL has been utilized to make specialists that can meta-learn ("figure out how to learn"), permitting them to sum up to complex visual conditions they have never seen before DRL stands to expand how much actual undertakings that can robotized by learn. Nonetheless, DRL doesn't stop there, as RL is an overall approach to moving toward streamlining issues by experimentation. From planning cutting edge machine interpretation models to developing new enhancement capabilities, DRL has previously been utilized to move toward every kind of AI assignment. Also, similarly, that deep learning has been used across many parts of AI, it appears to be logical that later on, DRL will be a significant part of developing general AI frameworks.

3.3. Parameter Selection

Finally, parameter selection of the RLCCA-SMSIP technique involves SCA for DRL model. The concept of SCA is easy and simple for the implementation process [19]. It adopts only the functions of sine and cosine properties to accomplish local development and global exploration of the problem and endlessly enhances the solution by using iteration development. Consider that there exists N search agent in the D-dimension search space, whereby the position of $i\text{-}th$ search agents are formulated by $x_i = (x_{i1}, x_{i2}, \cdots, x_{iD}), i \in \{1,2, \cdots, N\}$. The procedure is given in the following:

Initially, the location of N search agent is initialized randomly in the problem. Next, the fitness value is evaluated according to the decision criterion. Lastly, the present optimum individual location is saved and selected. In all the iterations, the individual update the location based on the following equation.

$$x_{id}^{t+1} = \begin{cases} x_{id}^t + r_1 \times \sin r_2 \times |r_3 P_d^t - x_{id}^t|, & r_4 < 0.5, \\ x_{id}^t + r_1 \times \cos r_2 \times |r_3 P_d^t - x_{id}^t|, & r_4 \geq 0.5, \end{cases} \quad (1)$$

In Eq. (1), t indicates the existing round, x_{id}^t represents the location of $i\text{-}th$ solutions in $d\text{-}th$ dimensions at $t\text{-}th$ rounds, and P_d^t indicates the location of global optimum in $d\text{-}th$ dimensions at $t\text{-}th$ rounds. There four major variables in (1), whereby $r_1 = 2(1 - t/T)$(T shows the maximal amount of rounds) is the sine-cosine amplitude adjustment factor, and r_1 describes the direction of following rounds of $i\text{-}th$ variables; $r_2 \in (0,2\pi)$, $r_3 \in (0,2)$, and $r_4 \in (0,1)$ epitomizes random number, where r_2 defines the distance for the following iterations of $i\text{-}th$ parameter, r_3 represents the weighted factor of the global optimum and r_4 denotes the discriminative coefficient.

4. Results and Discussion

The climate change classification results of the RLCCA-SMSIP model are examined under different dimensions. Fig. 3 depicts the confusion matrix accomplished by the RLCCA-SMSIP model on 70% of TR data. The RLCCA-SMSIP model has categorized 392 samples into C-1, 125 samples into C-2, 423 samples into C-3, 330 samples into C-4, 223 samples into C-5, 452 samples into C-6, and so on.

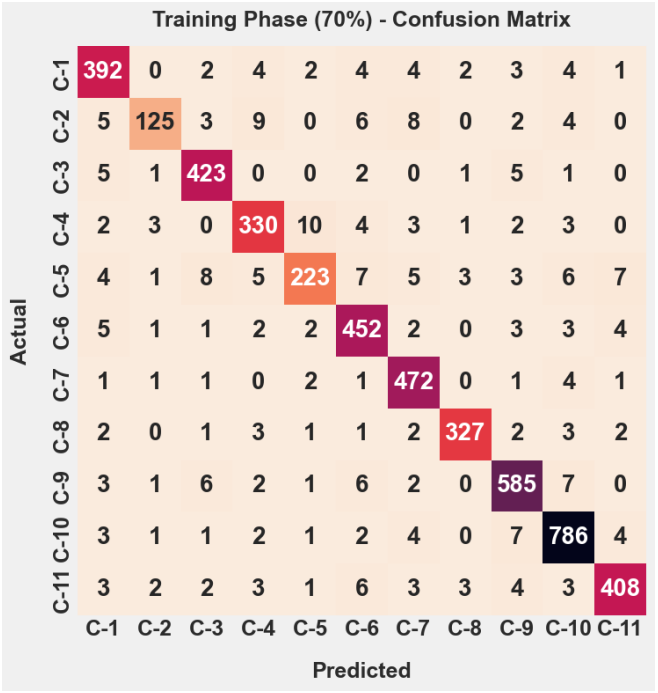

Figure 3. Confusion matrix of RLCCA-SMSIP approach under 70% of TR dataset

Table 1 and Figure. 4 demonstrate the overall climate change classification outcomes of the RLCCA-SMSIP model on 70% of climate data. The achieved results inferred the improvements of the RLCCA-SMSIP model. For instance, the RLCCA-SMSIP model has resulted in effectual outcomes with average $accu_y$, $prec_n$, $reca_l$, F_{score}, and MCC of 98.90%, 93.66%, 92.27%, 92.87%, and 92.32% respectively.

Table 1 Result analysis of RLCCA-SMSIP approach with distinct class labels under 70% of TR dataset

Training Phase (70%)					
Labels	**Accuracy**	**Precision**	**Recall**	**F-Score**	**MCC**
C-1	98.77	92.24	93.78	93.00	92.33
C-2	99.00	91.91	77.16	83.89	83.72
C-3	99.17	94.42	96.58	95.49	95.04
C-4	98.79	91.67	92.18	91.92	91.27
C-5	98.57	91.77	81.99	86.60	86.00
C-6	98.71	92.06	95.16	93.58	92.88
C-7	99.07	93.47	97.52	95.45	94.96
C-8	99.44	97.03	95.06	96.04	95.74
C-9	98.75	94.81	95.43	95.12	94.41
C-10	98.69	95.39	96.92	96.15	95.36
C-11	98.98	95.55	93.15	94.34	93.79
Average	**98.90**	**93.66**	**92.27**	**92.87**	**92.32**

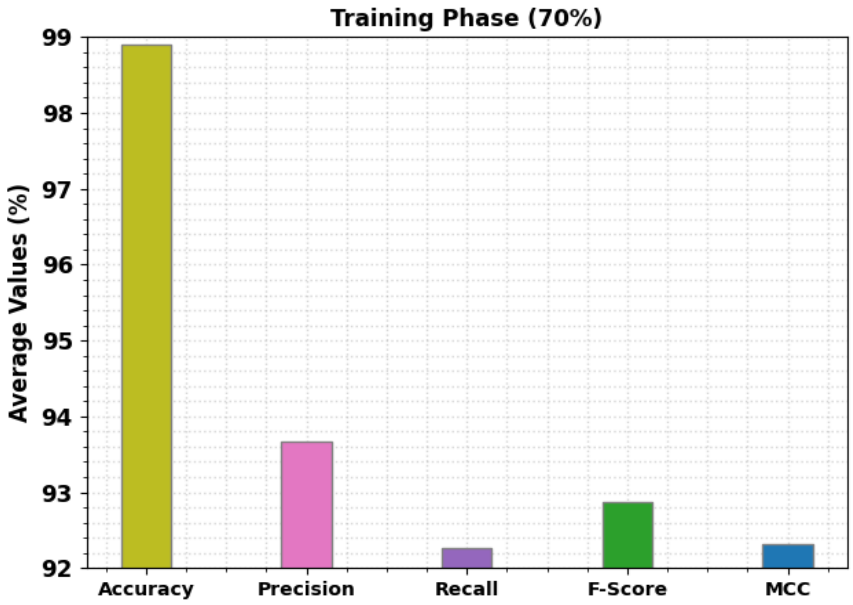

Figure 4. Average analysis of RLCCA-SMSIP approach under 70% of TR dataset

Figure. 5 portrays the confusion matrix accomplishes by the RLCCA-SMSIP technique on 30% of TS dataset. The RLCCA-SMSIP method has categorized 161 samples into C-1, 62 samples into C-2, 176 samples into C-3, 156 samples into C-4, 95 samples into C-5, 213 samples into C-6, and so on.

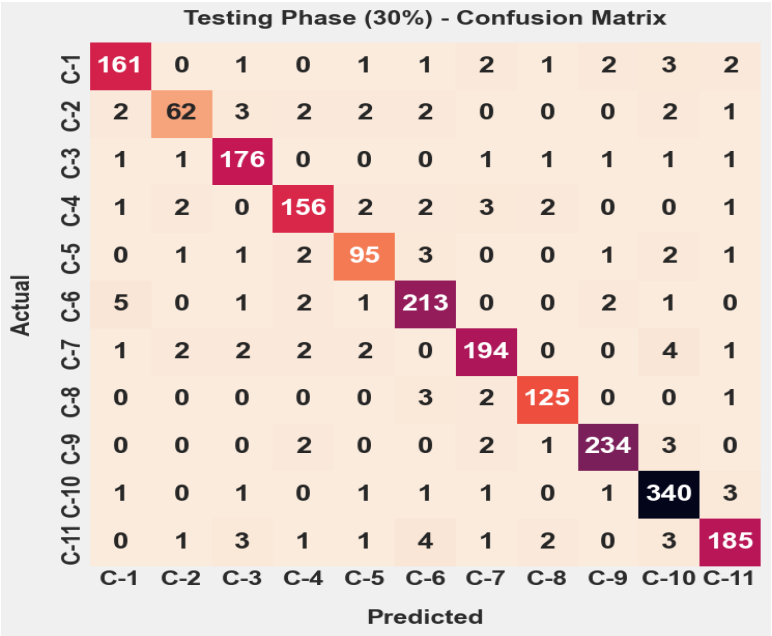

Figure 5. Confusion matrix of RLCCA-SMSIP approach under 30% of TS dataset

Table 2 and Fig. 6 validate the overall climate change classification outcomes of the RLCCA-SMSIP approach on 30% of climate data. The achieved results inferred the improvements of the RLCCA-SMSIP technique. For example, the RLCCA-SMSIP technique has resulted in effectual outcomes with average $accu_y$, $prec_n$, $reca_l$, F_{score}, and MCC of 98.92%, 93.55%, 92.88%, 93.19%, and 92.61% correspondingly.

Table 2 Result analysis of RLCCA-SMSIP approach with distinct class labels under 30% of TS dataset

	Testing Phase (30%)				
Labels	**Accuracy**	**Precision**	**Recall**	**F-Score**	**MCC**
C-1	98.84	93.60	92.53	93.06	92.43
C-2	98.98	89.86	81.58	85.52	85.10
C-3	99.08	93.62	96.17	94.88	94.38
C-4	98.84	93.41	92.31	92.86	92.23
C-5	98.98	90.48	89.62	90.05	89.51
C-6	98.64	93.01	94.67	93.83	93.08
C-7	98.74	94.17	93.27	93.72	93.02
C-8	99.37	94.70	95.42	95.06	94.72
C-9	99.27	97.10	96.69	96.89	96.48
C-10	98.64	94.71	97.42	96.05	95.24
C-11	98.69	94.39	92.04	93.20	92.48
Average	**98.92**	**93.55**	**92.88**	**93.19**	**92.61**

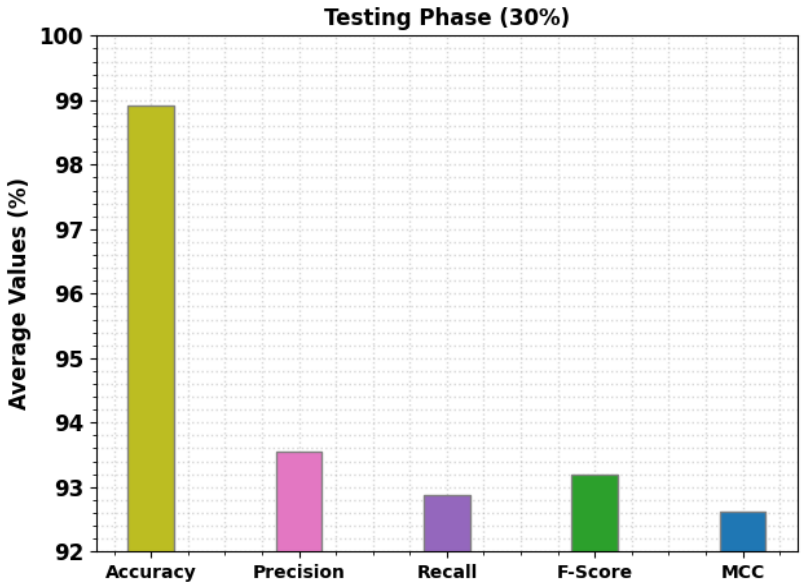

Figure 6. Average analysis of RLCCA-SMSIP approach under 30% of TS dataset

The training accuracy (TRA) and validation accuracy (VLA) acquired by the RLCCA-SMSIP approach on test dataset was showed in Fig. 7. The experimental outcome denotes the RLCCA-SMSIP technique has attained maximal values of TRA and VLA. In Particular, the VLA is greater than TRA.

The training loss (TRL) and validation loss (VLL) obtained by the RLCCA-SMSIP technique on test dataset are shown in Fig. 8. The experimental outcome implied that the RLCCA-SMSIP method has established least values of TRL and VLL. Particularly, the VLL is lesser than TRL.

Table 3 and Figure. 9 illustrate the climate classification results of the RLCCA-SMSIP model and other existing models. The experimental outcomes implied better results of the RLCCA-SMSIP model. For example, in terms of $prec_n$, the RLCCA-SMSIP model has provided increased $prec_n$ of 98.92% whereas the MeteCNN, VGG16, ResNet18, efficientNet-B7, and Mobilenetv3-small models have shown reduced $prec_n$ of 93.89%, 87.83%, 89.16%, 88.46%, and 85.26% respectively. Finally, in terms of $accu_y$, the RLCCA-SMSIP method has offered increased $accu_y$ of 93.19% whereas the MeteCNN, VGG16, ResNet18, efficientNet-B7, and Mobilenetv3-small techniques have shown reduced $accu_y$ of

92.42%, 87.33%, 88.52%, 87.68%, and 84.60% correspondingly. Therefore, the RLCCA-SMSIP model can be utilized for maximum climate classification process.

Figure 7. TRA and VLA analysis of RLCCA-SMSIP algorithm

Figure 8. TRL and VLL analysis of RLCCA-SMSIP algorithm

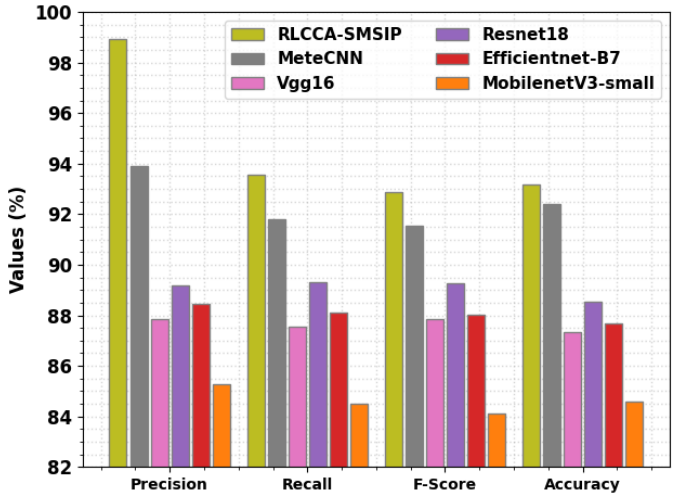

Figure 9. Comparative analysis of RLCCA-SMSIP approach recent algorithms

Table 3 Comparative analysis of RLCCA-SMSIP approach recent algorithms

Methods	Precision	Recall	F-Score	Accuracy
RLCCA-SMSIP	98.92	93.55	92.88	93.19
MeteCNN	93.89	91.82	91.56	92.42
Vgg16	87.83	87.54	87.85	87.33
Resnet18	89.16	89.29	89.27	88.52
Efficientnet-B7	88.46	88.10	88.04	87.68
MobilenetV3-small	85.26	84.51	84.10	84.60

5. Conclusion

In this paper, a new RLCCA-SMSIP technique is developed for climate classification. In order to properly determine climate change, the RLCCA-SMSIP technique employs ResNet-101 model for feature extraction. Next, the DRL approach is utilized for climate classification. Finally, parameter selection of the RLCCA-SMSIP technique involves SCA for DRL model. For assuring the enhanced outcomes of the presented RLCCA-SMSIP model, comprehensive comparison results are assessed. The obtained values denote the supremacy of the RLCCA-SMSIP model on climate classification.

Acknowledgements

Funding

This research did not receive any specific grant from funding agencies in the public.

Authors' contributions

All authors contributed toward data analysis, drafting, and revising the paper and agreed to be responsible for all the aspects of this work.

Declaration of Conflicts of Interests

Authors declare that they have no conflict of interest.

Declarations

Author(s) declare that all works are original and this manuscript has not been published in any other journal.

References

[1] Asokan, A. and Anitha, J., 2019, February. Machine learning based image processing techniques for satellite image analysis-a survey. In *2019 International conference on machine learning, big data, cloud and parallel computing (COMITCon)* (pp. 119-124). IEEE.

[2] Chen, Z., Jia, K., Xiao, C., Wei, D., Zhao, X., Lan, J., Wei, X., Yao, Y., Wang, B., Sun, Y. and Wang, L., 2020. Leaf area index estimation algorithm for GF-5 hyperspectral data based on different feature selection and machine learning methods. *Remote Sensing*, *12*(13), p.2110.

[3] Gómez, D., Salvador, P., Sanz, J. and Casanova, J.L., 2019. Potato yield prediction using machine learning techniques and sentinel 2 data. *Remote Sensing*, *11*(15), p.1745.

[4] Li, Y., Li, C., Li, M. and Liu, Z., 2019. Influence of variable selection and forest type on forest aboveground biomass estimation using machine learning algorithms. *Forests*, *10*(12), p.1073.

[5] Ahmadi, K., Kalantar, B., Saeidi, V., Harandi, E.K., Janizadeh, S. and Ueda, N., 2020. Comparison of machine learning methods for mapping the stand characteristics of temperate forests using multi-spectral sentinel-2 data. *Remote Sensing*, *12*(18), p.3019.

[6] Hosseini, F.S., Choubin, B., Mosavi, A., Nabipour, N., Shamshirband, S., Darabi, H. and Haghighi, A.T., 2020. Flash-flood hazard assessment using ensembles and Bayesian-based machine learning models: application of the simulated annealing feature selection method. *Science of the total environment*, *711*, p.135161.

[7] Arjasakusuma, S., Swahyu Kusuma, S. and Phinn, S., 2020. Evaluating variable selection and machine learning algorithms for estimating forest heights by combining lidar and hyperspectral data. *ISPRS International Journal of Geo-Information*, *9*(9), p.507.

[8] Thwal, N.S., Ishikawa, T. and Watanabe, H., 2019, October. Land cover classification and change detection analysis of multispectral satellite images using machine learning. In *Image and Signal Processing for Remote Sensing XXV* (Vol. 11155, pp. 522-532). SPIE.

[9] Ferreira, B., Iten, M. and Silva, R.G., 2020. Monitoring sustainable development by means of earth observation data and machine learning: A review. *Environmental Sciences Europe*, *32*(1), pp.1-17.

[10] Balogun, A.L., Yekeen, S.T., Pradhan, B. and Althuwaynee, O.F., 2020. Spatio-temporal analysis of oil spill impact and recovery pattern of coastal vegetation and wetland using multispectral satellite landsat 8-OLI imagery and machine learning models. *Remote Sensing*, *12*(7), p.1225.

[11] Verma, P. and Patil, S., 2022. Machine Learning for Cloud Cover Detection Using Multispectral Satellite Images. *Annals of Data Science*, pp.1-15.

[12] Wang, Y., Su, J., Zhai, X., Meng, F. and Liu, C., 2022. Snow coverage mapping by learning from sentinel-2 satellite multispectral images via machine learning algorithms. *Remote Sensing*, *14*(3), p.782.

[13] Fu, B., Zuo, P., Liu, M., Lan, G., He, H., Lao, Z., Zhang, Y., Fan, D. and Gao, E., 2022. Classifying vegetation community's karst wetland synergistic use of image fusion and object-based machine learning algorithm with Jilin-1 and UAV multispectral images. *Ecological Indicators*, *140*, p.108989.

[14] Oliveira, R.P.D., Barbosa Júnior, M.R., Pinto, A.A., Oliveira, J.L.P., Zerbato, C. and Furlani, C.E.A., 2022. Predicting Sugarcane Biometric Parameters by UAV Multispectral Images and Machine Learning. *Agronomy*, *12*(9), p.1992.

[15] Li, X., Lin, H., Long, J. and Xu, X., 2021. Mapping the growing stem volume of the coniferous plantations in North China using multispectral data from integrated GF-2 and Sentinel-2 images and an optimized Feature variable selection method. *Remote Sensing*, *13*(14), p.2740.

[16] Pontoglio, E., Dabove, P., Grasso, N. and Lingua, A.M., 2021. Automatic features detection in a fluvial environment through machine learning techniques based on UAVs multispectral data. *Remote Sensing*, *13*(19), p.3983.

[17] Zhang, Q., 2022. A novel ResNet101 model based on dense dilated convolution for image classification. *SN Applied Sciences*, *4*(1), pp.1-13.

[18] Degrave, J., Felici, F., Buchli, J., Neunert, M., Tracey, B., Carpanese, F., Ewalds, T., Hafner, R., Abdolmaleki, A., de Las Casas, D. and Donner, C., 2022. Magnetic control of tokamak plasmas through deep reinforcement learning. *Nature*, *602*(7897), pp.414-419.

[19] Pande, S. D., Kanna, R. K., & Qureshi, I. (2022). Natural Language Processing Based on Name Entity With N-Gram Classifier Machine Learning Process Through GE-Based Hidden Markov Model. Machine Learning Applications in Engineering Education and Management, 2(1), 30–39.

[20] Eslami, M., Neshat, M. and Khalid, S.A., 2022. A novel hybrid sine cosine algorithm and pattern search for optimal coordination of power system damping controllers. *Sustainability*, *14*(1), p.541.

[21] Morzelona, R. (2021). Human Visual System Quality Assessment in The Images Using the IQA Model Integrated with Automated Machine Learning Model. Machine Learning Applications in Engineering Education and Management, 1(1), 13–18.
[22] Sherje, D. N. . (2021). Content Based Image Retrieval Based on Feature Extraction and Classification Using Deep Learning Techniques. Research Journal of Computer Systems and Engineering, 2(1), 16:22.
[23] Jat, N. C., & Kumar, C. (2022). Design assessment and simulation of PCA based image difference detection and segmentation for satellite images using machine learning. International Journal on Recent and Innovation Trends in Computing and Communication, 10(3), 1-11. doi:10.17762/ijritcc.v10i3.5520
[24] Nithya, S., and Moses, M., 2021. Geographical Information System (GIS) based Energy Station Identification and Frequency Analysis Using ETAP: A Sample Real Time Test Case System in INDIA. *International Journal of Applied Engineering and Technology*, 3(1), pp.1-6.
[25] Mr. Kaustubh Patil. (2013). Optimization of Classified Satellite Images using DWT and Fuzzy Logic. International Journal of New Practices in Management and Engineering, 2(02), 08 - 12.